Transcription factor *AtMYB103* is required for anther development by regulating tapetum development, callose dissolution and exine formation in Arabidopsis

Zai-Bao Zhang[1,2,†], Jun Zhu[1,†], Ju-Fang Gao[1,†], Chen Wang[1], Hui Li[1], Hong Li[3], Hui-Qi Zhang[1], Sen Zhang[1], Dong-Mi Wang[4], Quan-Xi Wang[1], Hai Huang[3], Hui-Jun Xia[2] and Zhong-Nan Yang[1,*]

[1]*College of Life and Environmental Sciences, Shanghai Normal University, Shanghai 200234, China,*

[2]*Key Laboratory of MOE for Plant Developmental Biology, College of Life Sciences, Wuhan University, Wuhan, Hubei 430072, China,*

[3]*Shanghai Institute of Plant Physiology and Ecology, Chinese Academy of Sciences, Shanghai 200032, China, and*

[4]*Forestry Bureau of Taizhou City, Zhejiang 318020, China*

Summary

Downregulation of the transcription factor *AtMYB103* using transgenic technology results in early tapetal degeneration and pollen aberration during anther development in *Arabidopsis thaliana*. This paper describes the functional analysis of the *AtMYB103* gene in three knock-out mutants. Two male sterile mutants, *ms188-1* and *ms188-2*, were generated by ethyl-methane sulfonate (EMS) mutagenesis. A map-based cloning approach was used, and *ms188* was mapped to a 95.8-kb region on chromosome 5 containing an *AtMYB103* transcription factor. Sequence analysis revealed that *ms188-1* had a pre-mature stop codon in the *AtMYB103* coding region, whereas *ms188-2* had a CCT → CTT base-pair change in the first exon of *AtMYB103*, which resulted in the replacement of a proline by a leucine residue in the R2R3 domain. The third mutant, an *AtMYB103* transposon-tagging line, also showed a male sterile phenotype. Allelism tests indicated that *MS188* and *AtMYB103* belong to the same locus. Cytological observation revealed defective tapetum development and altered callose dissolution in *ms188* plants. Additionally, most of the microspores in mature anthers were degraded and surviving microspores lacked exine. *AtMYB103* encoded an R2R3 MYB protein that is predominantly located in the nucleus. Real-time RT-PCR analysis indicated that the callase-related gene *A6* was regulated by *AtMYB103*. Expression of the exine formation gene *MS2* was not detected in mutant anthers. These results implicate that *AtMYB103* plays an important role in tapetum development, callose dissolution and exine formation in *A. thaliana* anthers.

Keywords: Arabidopsis, transcription factor, male sterility, tapetum, exine wall, callase.

Introduction

Angiosperm pollen development consists of two sequential phases: microsporogenesis and microgametogenesis. Both phases occur within the anther locule, which is lined by a tapetal cell layer (tapetum). Microsporogenesis is initiated upon meiotic division of the diploid pollen mother cell (PMC), which produces the four haploid microspores that comprise a tetrad. During microgametogenesis, microspores released from the tetrads undergo cell expansion, cell wall synthesis, asymmetric division, and differentiation of the vegetative and generative cells before being released from the anther. The tapetal cells play a major role in pollen development by contributing to microspore release, nutrition, pollen wall synthesis and pollen coat deposition (Goldberg *et al.*, 1993). Both the release of microspores from tetrads and exine formation are critical processes in pollen development.

Cell wall formation and dissolution is a unique feature of male meiosis in plants during and after meiotic division. The

tetrad cell wall (callose wall) is composed mainly of β-1, 3-glucans. The individual microspores are released at the end of meiosis when the callose wall is dissolved by a mixture of enzymes (callases) secreted by the tapetum (Steiglitz and Stern, 1973). β-1,3-Glucanases are a diverse family of hydrolytic enzymes that are classified as endoglucanases or exoglucanases depending upon the nature of their enzymatic action. Endoglucanases cleave β-1,3-glucans into short-chain reducing sugars, whereas exoglucanase hydrolysis releases single glucose units from the reducing ends of the substrate. In *Lilium*, endo-β-1,3-glucanase was shown to be responsible for callose wall degradation. The majority of endoglucanase activity occurs in the tapetum, immediately surrounding meiocytes, whereas the majority of exoglucanase activity occurs in the outer somatic layers of the anther (Steiglitz, 1977).

Several candidate genes encoding the endo-β-1,3-glucanase component of callase have been reported. Sequence similarity studies have suggested that *Tag1* from tobacco encodes a β-1,3-glucanase. It is expressed selectively in the tapetum, with maximal expression just prior to tetrad dissolution, and represents a novel β-1,3-glucanase class based on phylogenetic analysis and RNA expression pattern (Bucciaglia and Smith, 1994). In Arabidopsis, the *A6* gene encodes a protein similar to β-1,3-glucanase. Although the size of the A6 protein suggests it to be an exoglucanase, the A6 sequence shows significant amino acid similarity to endoglucanases (Hird *et al.*, 1993). Recent research has suggested that in transgenic tobacco, the expression of the *A6* promoter was restricted to the anther, and the phenotypic effect of *A6-barnase* expression was tapetal ablation and male sterility (Hird *et al.*, 1993). Although the temporal and spatial expression of these genes is associated with tetrad dissolution, their roles in the release of microspores from the tetrads and in the regulation of callose dissolution has not been fully elucidated.

In most plant species, the pollen grain wall is composed of an inner layer (intine) and an outer layer (exine). The exine plays an important role in protecting pollen from various environmental stresses and bacterial attacks, and in cell–cell recognition. The exine wall is frequently decorated with complex patterns of spines and ridges, and is composed primarily of sporopollenin, which is extremely resistant to decay, and is formed by a series of related polymers derived from long-chain fatty acids as well as modest amounts of oxygenated aromatic rings and phenylpropanoids (Piffanelli *et al.*, 1998). During the tetrad stage, a cellulose matrix (primexine) accumulates between the microspore plasma membrane and the callose wall, and serves as a scaffold for sporopollenin deposition, from which the probacula and tectum are subsequently formed (Fitzgerald and Knox, 1995; Heslop-Harrison, 1963). Upon degeneration of the callose wall, microspores are released into the locule, and the bacula and tectum continue to increase in size. At the bicellular pollen stage, the reticulate pattern of the exine is almost complete, and the pollen grain is surrounded by a sculptured exine wall (Scott *et al.*, 2004).

Several Arabidopsis mutants with exine defects have been isolated and characterized. The *MS2* gene encodes a putative fatty acid reductase that catalyzes fatty acyl groups to fatty alcohol groups and participates in sporopollenin synthesis. The *ms2* plants exhibited male sterility with pollen lacking exine formation (Aarts *et al.*, 1993, 1997). The *DEX1* gene was shown to be required for exine pattern formation during pollen development in Arabidopsis. The DEX1 protein could be a component of either the primexine matrix or the endoplasmic reticulum, and might participate in primexine precursor assembly (Paxson-Sowders *et al.*, 2001). The *flp1* mutant has microspores with an altered exine: the pollen surface is nearly smooth. This protein appears to be a transporter or a catalytic enzyme involved in fatty acid biosynthesis, which is necessary for both sporopollenin and wax crystals synthesis (Ariizumi *et al.*, 2003). The *NEF1* gene encodes a membrane protein, and its disruption has been shown to affect lipid accumulation in the tapetum plastid, primexine formation and sporopollenin synthesis. Additionally, no exine formation was observed in *nef1* mutants (Ariizumi *et al.*, 2004). Although analysis of these mutants has contributed significantly to the study of pollen exine development, the regulatory mechanisms involved in this process are yet to be elucidated.

Regulation of gene expression by transcription factors influences many biological processes in cells and organisms. Transcription factors are categorized into families based on their structure and target DNA binding sequences. In plants, the MYB family is one of the largest groups of transcription factors. To date, a total of nine MYB genes specifically expressed in anthers have been identified, including *AID1* in rice (Zhu *et al.*, 2004), *ZmMYBP2* in maize (Zhang *et al.*, 2000), *NtMYBAS1* and *NtMYBAS2* in tobacco (Yang *et al.*, 2001), and *AtMYB33*, *AtMYB65* (Millar and Gubler, 2005), *AtMYB26* (Steiner-lange *et al.*, 2003), *AtMYB32* (Preston *et al.*, 2004) and *AtMYB103* (Higginson *et al.*, 2003; Li *et al.*, 1999) in Arabidopsis. *AtMYB103* is expressed in anthers and trichomes. Antisense knock-down of *AtMYB103* altered pollen, tapetum and trichome development. Additionally, in antisense lines, pollen grains were distorted in shape with reduced or no cytoplasmic content, tapetum degenerated earlier in development, and trichomes on cauline and rosette leaves produced additional branches and contained more nuclear DNA than wild-type trichomes (Higginson *et al.*, 2003; Li *et al.*, 1999). The role of *AtMYB103* in anther development has not, however, been fully elucidated.

In the current study, we explored as yet undescribed functions of *AtMYB103* in Arabidopsis anther development utilizing *AtMYB103* knock-out plants. Cytological analysis was employed to examine the effects of *AtMYB103* mutation

on tapetum development, callose wall degradation and exine formation. RT-PCR and real-time RT-PCR were used to reveal key genes responsible for callose dissolution and exine development. A discussion of the relevance of the results with respect to the role *AtMYB103* in pollen development in Arabidopsis is included.

Results

Isolation and identification of ms188 *mutants*

Screening of a mutant population of Arabidopsis ecotype Landsberg *erecta* generated by ethyl-methane sulphonate (EMS) mutagenesis revealed two male sterile mutants (Figure 1). Both mutants exhibited normal vegetative and floral development, with the exception of the male sterile phenotype. In order to examine the segregation ratio of the male-sterility phenotype, mutants were crossed with wild-type plants. The F1 plants showed normal fertility, and the fertility and sterility of plants in the F2 population segregated in a 3:1 ratio for both mutants, suggesting that the inherited male sterile phenotype was a single recessive Mendelian locus. Genetic complementation indicated that both mutants were altered at the same locus and were consequently named *ms188-1* and *ms188-2*; *ms188-1* was used for gene mapping. Given that both had similar phenotypes, *ms188-1* was used for further analysis unless specifically indicated.

Isolation of the MS188 *gene using a map-based cloning strategy*

A map-based cloning approach was used to identify the *MS188* gene in a population generated from a cross between *ms188-1* and an Arabidopsis ecotype Columbia. A total of 25 In/Del and SSLP markers were used for first-pass mapping (Table S1) (Jander *et al.*, 2002). *MS188* was linked to the MCO15 In/Del marker on chromosome 5. A population containing more than 2000 male sterile progeny was used for subsequent fine mapping of this gene, and *MS188* was mapped to a 95.8-kb region between In/Del markers K24C1 and MDA7 on chromosome 5 (Figure 2a). A total of 18 In/Del markers (Table S2) were developed for the mapping of *MS188*, utilizing the Cereon database (http://www.arabidopsis.org).

The identified region contained 28 genes, including an *AtMYB103* transcription factor. Previous research suggested that the *AtMYB103* gene was highly expressed in anther, and that its downregulation affected the shape of pollen grains during anther development in *Arabidopsis thaliana* (Higginson *et al.*, 2003; Li *et al.*, 1999). Consequently, we sequenced the genomic region of this gene from *ms188-1* and wild-type ecotype L*er*. A CAA → TAA base-pair change in the second exon of *AtMYB103* was identified in the *ms188-1* mutant, resulting in premature termination of translation. The genomic region of this gene from the *ms188-2* mutant line was then sequenced. We identified a CCT → CTT base-pair change in the first exon of *AtMYB103* that resulted in the replacement of a proline by a leucine residue in the R2R3 domain of the mutant protein (Figure 2b). Sequence analysis of both mutants suggested that *AtMYB103* might be the candidate *MS188* gene.

Genetic complementation was performed to validate the *AtMYB103* gene. A database search showed a transposon tagging line of *AtMYB103* (*pst00809*) in the mutant collection in RIKEN (http://rarge.gsc.riken.jp) (Seki *et al.*, 1998, 2002). A Ds element was inserted in the second intron of *AtMYB103* in *pst00809*, and this line also displayed a male sterile phenotype. When it was used as a female parent in a cross
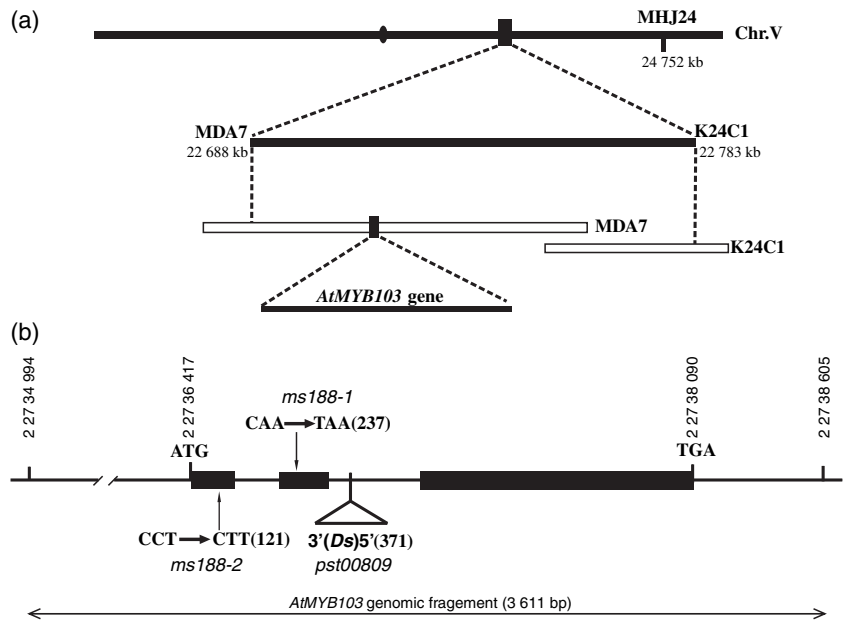

Figure 1. Phenotypes of wild-type (L*er*), *ms188-1* mutant and transgenic plants for complementation.
(a) A wild-type plant with fertility indicated by siliques with normal seed set.
(b) An *ms188-1* mutant plant. Mutants resembled wild-type plants, with the exception that the siliques remained undeveloped and were devoid of seeds.
(c) An *AtMYB103* transgene plant with *ms188-1* homozygous background showing normal fertility.
(d) A wild-type flower, showing anthers with pollen grains.
(e) An *ms188-1* flower, showing anthers without pollen grains.

Figure 2. Molecular identification of the *At-MYB103* gene.
(a) Fine mapping of *ms188-1* to a 95.8-kb region between In/Del markers K24C1 and MDA7 on chromosome 5.
(b) The *AtMYB103* gene structure and positions of the nucleotide changes in *ms188-1*, *ms188-2* and *Ds* insertion mutant *pst00809*. Black boxes indicate *AtMYB103* exons. The double-arrow line indicates the *AtMYB103* genomic fragment used for the complementation of *ms188-1*. The numbers indicate the positions of the start and stop nucleotides of the fragments located on the genome.

with *ms188-1* heterozygous plants, the F1 plants from the crosses segregated as 1:1 (fertile:sterile), suggesting *MS188* was an allele of *AtMYB103*, and that *AtMYB103* mutations resulted in the male sterile phenotype in *ms188* mutants.

A complementation experiment was also performed. A 3611-bp genomic DNA fragment including the predicted promoter, transcription region and the 3′ untranslated region of *AtMYB103* was cloned and introduced into the *ms188* heterozygous plants (Figure 2b). Thirty-five independent transgenic plants were obtained in the screen. Two lines with *ms188* homozygous backgrounds were identified using closely linked molecular markers (data not shown). These two lines showed the wild-type phenotype with normal fertility (Figure 1c). This result demonstrates that male sterility can be restored by the 3611-bp fragment of the *AtMYB103* gene. Therefore, both the genetic complementation and the molecular complementation experiments indicate that mutation within the *AtMYB103* was responsible for the *ms188* phenotype.
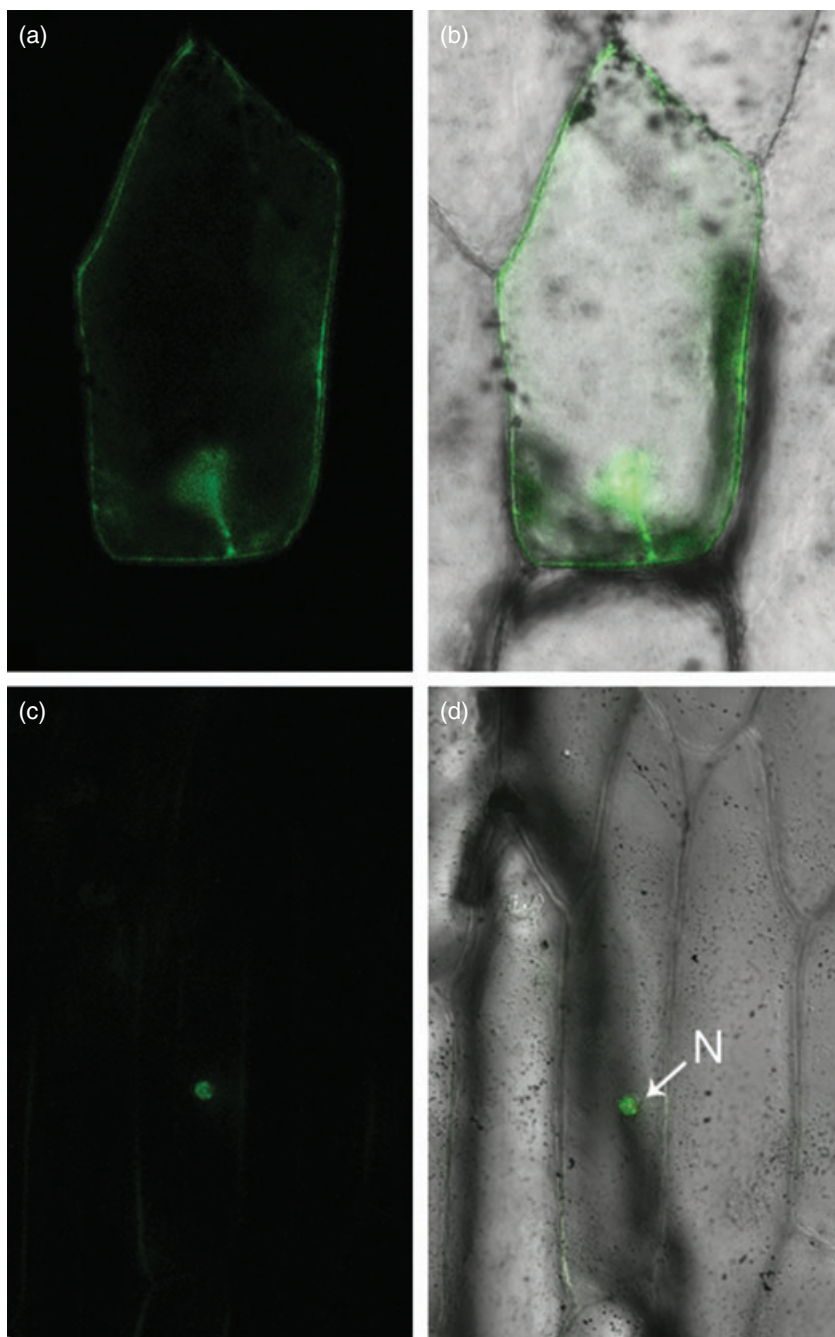
AtMYB103 protein is localized to the nucleus

AtMYB103 encodes a 321 amino acid protein with a molecular mass of 36 kDa that contained an N-terminal MYB DNA-binding domain. This domain is composed of two repeats, of about 53 amino acids, from amino acid positions 12–115; each forming a helix-turn-helix structure and consequently belonging to the R2R3-type of MYB transcription factors (Li *et al.*, 1999). BLAST searches showed limited similarity between AtMYB103 and a number of proteins that contained R2R3 domains in Arabidopsis, including MYB26, MYB32, MYB33 and MYB65; these R2R3-containing proteins are required for pollen development (Figure S1). Some MYB members, such as *NtMYBAS* (Yang *et al.*, 2001), display nuclear localization signals (NLS) and have been shown to function as transcription factors. However, no conventional NLS domain was predicted in *AtMYB103*. Translational fusion of AtMYB 103 to GFP driven by the 35S promoter was constructed to determine whether AtMYB103 is localized to the nucleus (Figure 3c and d). In control bombardments with the vector alone, GFP was found throughout the cell (Figure 3a and b). Introduction of the AtMYB103-GFP fusion protein into onion epidermal cells by particle bombardment resulted in nuclear localization of the fluorescence signal, a finding that is consistent with a transcription regulatory role for AtMYB103.

AtMYB103 controls tapetum development, callose dissolution and exine formation

To further elucidate the biological functions of *AtMYB103* in anther development, anthers of both *ms188-1* and wild-type plants were examined by light microscopy. In Arabidopsis, anther development is divided into 14 stages based on morphological landmarks of cellular events (Sanders *et al.*, 1999). From stage 1 to stage 6, no detectable differences in anther development were observed between the *ms188-1* mutant and wild-type plants (data not shown). At stage 7, microspore mother cells completed meiosis and formed tetrads, which were surrounded by a callosic wall in wild-type plants (Figure 4a). The cell walls of the tapetal cells gradually degraded as the tapetum was transformed into the polar secretory type (Stevens and Murray, 1981), and were no longer observed after stage 7 (Figure 4b and c). In contrast, mutant tapetal cell walls remained intact and visible (Figure 4d–f). Wild-type tapetal cell protoplasts were still

Figure 3. Nuclear localization of AtMYB103-GFP fusion proteins. Onion epidermal cells were bombarded with pCAMBIA1302-AtMYB103-GFP and a control construct, pCAMBIA1302.
(a and b) The GFP protein was distributed throughout the cytoplasm and nucleus of control cells.
(c and d) The AtMYB103-GFP fusion protein was detected only in the nucleus (N).

visible at stage 11 (Figure 4c), whereas those of mutant tapetal cells were almost completely degenerated at this stage (Figure 4f). Thus, the knock-out of *AtMYB103* resulted in defects of tapetal cell wall degradation and tapetal cell protoplast degeneration during tapetum development.

Transverse sections also showed abnormal microspore development in mutants after stage 7. During the uninucleated stage (stages 8–10), microspores were released from the tetrads and covered with an exine wall in the wild-type anthers. In contrast, most of the mutant microspores

underwent degradation during this phase (Figure 4e). At stage 11, wild-type microspores were densely stained, indicating that they had become mature uninucleated pollen grains and had initiated mitotic divisions. Meanwhile, surviving microspores in mutants were shrunken and vacuolated (Figure 4f).

In anther development, microspores are released from tetrads after callose dissolution by callase, which is secreted from the tapetum (Steiglitz and Stern, 1973). Given that *AtMYB103* knock-out affected tapetum development, we
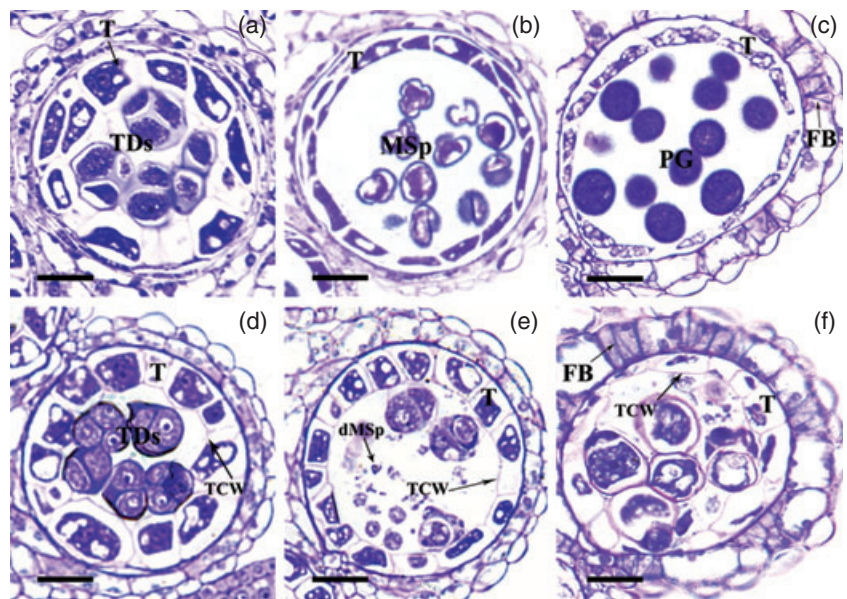
Figure 4. Cytological observation of anther and pollen development of wild-type (a–c) and *ms188* plants (d–f). (a and d) Tetrad stage.
(a) The tapetum cytoplasm was shrunken and the tapetal cell wall had begun to dissolve in wild-type plants.
(d) The tapetal cell walls of the mutant remained intact.
(b and e) Uninucleate microspore stage. Most *ms188* microspores were degraded in the locule. Tapetal cell walls of mutants were clearly visible.
(c and f) Mitosis pollen stage. The surviving microspores of *ms188* fused together in the locule, which also displayed a shrunken cytoplasm. The degeneration of the protoplast of the mutant tapetal was more severe than that noted in the wild type, and its cell wall persisted. FB, fibrous bands; dMSp, degraded microspores; MSp, microspores; T, tapetum; TCW, tapetal cell wall; Tds, tetrads. Scale bars = 20 μm.

Figure 5. Cytochemical staining for callose in wild-type and mutant anthers with aniline blue.
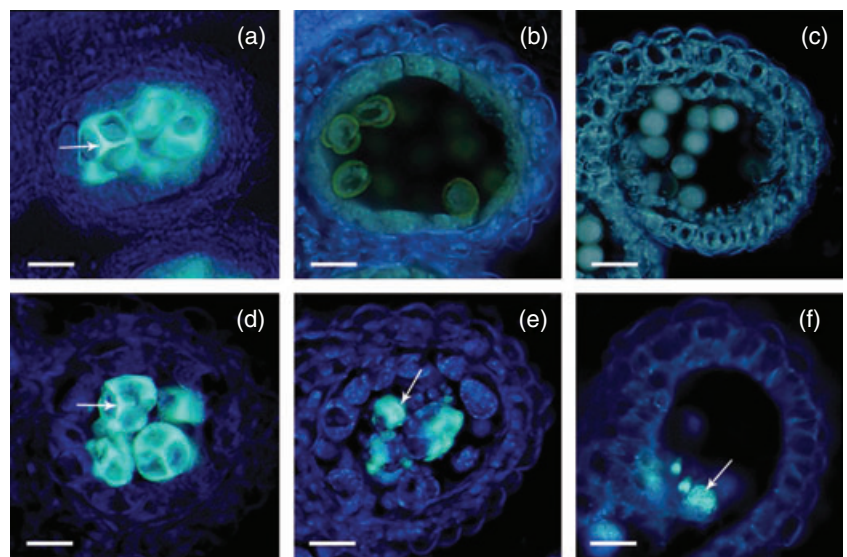(a–c) Fluorescence expression in wild-type anther with aniline blue staining under UV light.
(a) Anther section at stage 7, showing the tetrad surrounded with callose (white arrow).
(b and c) Anther section after stage 7, showing no callose detected in locules. (d–f) Aniline blue staining on a section of mutant anthers.
(d) Stage 7 of mutant anther, fluorescence expression was similar to that of wild-type plants (white arrow).
(e) Stage 9: decreased fluorescence relative to the tetrad stage was noted, indicating that the callose was partially degraded in mutant anthers (white arrow).
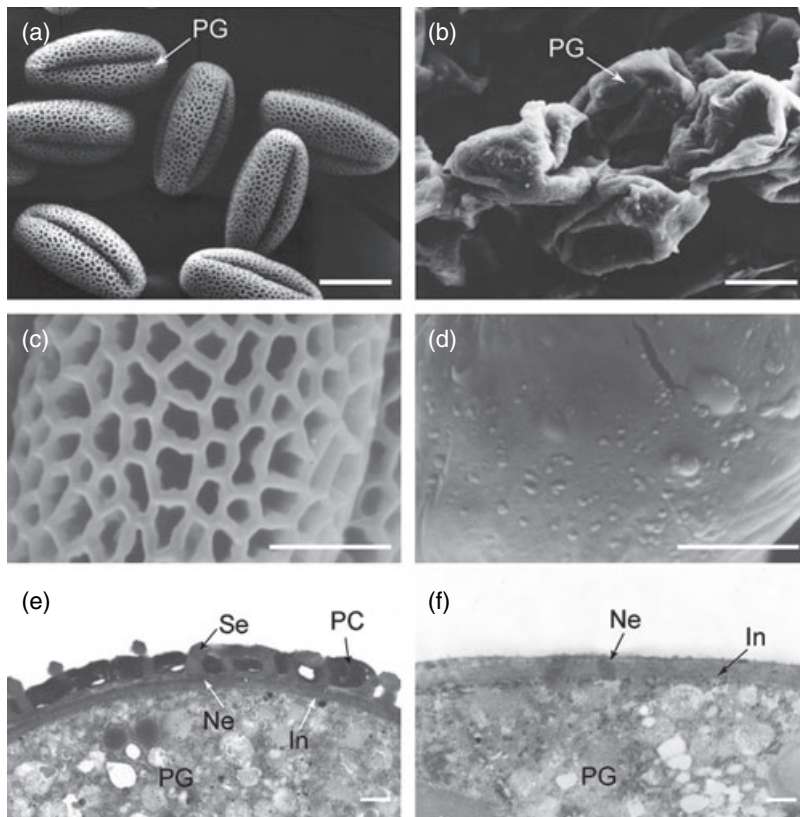(f) Dehiscence stage: fluorescence remained detectable in the mutant anther (white arrow). Scale bars = 20 μm.

utilized aniline blue staining to test whether callose degradation was altered in *ms188* mutants. Callose was not detected in the wild-type anther locules after stage 7 (Figure 5b and c). However, in *ms188-1* anthers, callose was observed from stage 7 to stage 12, with fewer noted during the later stages compared with stage 7 (Figure 5d–f). These data suggested *AtMYB103* affects callose dissolution, although it was partially degraded during the late stages of mutant anther development.

During anther development the tapetum provides materials for pollen wall synthesis (Steer, 1977). Although most microspores were degraded during the late stage of anther development, there were still a few pollen grains in the locules of *ms188-1*. Therefore, we further observed the pollen wall of wild-type and mutant lines to investigate the affects of *AtMYB103* on exine formation and structure. A regular reticulate pattern was observed in wild-type mature pollen grains (Figure 6a and c). Although pollen grains were observed in the mutant anther locules, scanning electron microscopy (SEM) revealed that they had an abnormally smooth surface (Figure 6b and d). The exine of wild-type pollen grains, including sexine and nexine, were evident by transmission electron microscopy (TEM) (Figure 6e), whereas mutant pollen grains were completely devoid of sexine (baculum and tectum) (Figure 6f). The pollen coat, mainly derived from the tapetum, filled the interstices of wild-type exine (Figure 6e), whereas no pollen coat was observed in the mutant locule (Figure 6f). These results

Figure 6. SEM and TEM micrographs of mature pollen from wild-type and *ms188* plants.
(a and c) SEM micrographs of wild-type mature pollen showed a regular reticulate pattern of pollen exine, whereas the *ms188* mutant displayed a smooth surface of pollen grains (b and d).
(e and f) TEM micrographs of wild-type mature pollen showed the exine layer, whereas no exine layer was observed on the pollen of sterile anthers. PC; pollen coat; PG, pollen grains; In, intine; Ne, nexine; Se, sexine. Scale bars = 10 μm (a and b), 5 μm (c and d) and 500 nm (e and f), respectively.

indicate that *AtMYB103* controls pollen exine formation in anther development.

AtMYB103 *acts upstream of* A6 *and* MS2

β-1,3-Glucanase is encoded by a gene family containing approximately 80 members in Arabidopsis. A total of 12 genes that are highly expressed in Arabidopsis anther according to gene expression information in the Genevestigator database (http://www.genevestigator.ethz.ch) were chosen for RT-PCR analysis. Of the 12 examined genes, only the expression of the *A6* gene was altered (Figure 7a). In order to further confirm the RT-PCR result, real-time RT-PCR analysis was performed. The expression levels of the *A6* gene in *ms188-1* and *pst00809* were only 9.2% and 7.6% of the wild-type expression level, respectively (Figure 7c). Therefore, both RT-PCR and real-time RT-PCR analysis indicated that *A6* was downregulated in *ms188* suggesting *AtMYB103* acting upstream of *A6*.

In Arabidopsis, four genes (*MS2*, *FLP1*, *DEX1* and *NEF1*) were reported to be involved in sporopollenin synthesis and exine pattern formation (Aarts *et al.*, 1997; Ariizumi *et al.*, 2003, 2004; Paxson-Sowders *et al.*, 2001). These genes were chosen for RT-PCR analysis to identify whether they are regulated by *AtMYB103*. Although the expression of *FLP1*, *DEX1* and *NEF1* genes was unchanged in *ms188-1*, *MS2*

expression was barely detectable in the mutant (Figure 7b). Real-time RT-PCR confirmed these results (Figure 7d). Real-time RT-PCR analysis of the expression of *AtMYB103* in the *ms2* mutant revealed that it was not dramatically different from that in wild-type, indicating that *MS2* was not responsible for the reduced expression of *AtMYB103* in the mutant (Figure 7e). All these results are consistent with *AtMYB103* acting upstream of *MS2* in anther development.

Discussion

The *AtMYB103* gene is a member of the R2R3 MYB gene family. Detailed gene expression has been investigated using RT-PCR, *in situ* hybridization and promoter-GUS analysis techniques (Higginson *et al.*, 2003; Li *et al.*, 1999). Downregulation of this gene has been shown to result in distortion of pollen grain shape and reduction of cytoplasmic content. Additionally, transgenic antisense lines showed reduced fertility (Higginson *et al.*, 2003). In the current paper, we have further extended the functions of this gene in Arabidopsis anther through cytological observation and molecular characterization of three knock-out mutants, *ms188-1*, *ms188-2* and *pst00809*. The knock-out of this gene resulted in a complete male sterile phenotype. Our data demonstrated a crucial role for *AtMYB103* in tapetum development, callose dissolution and exine formation.

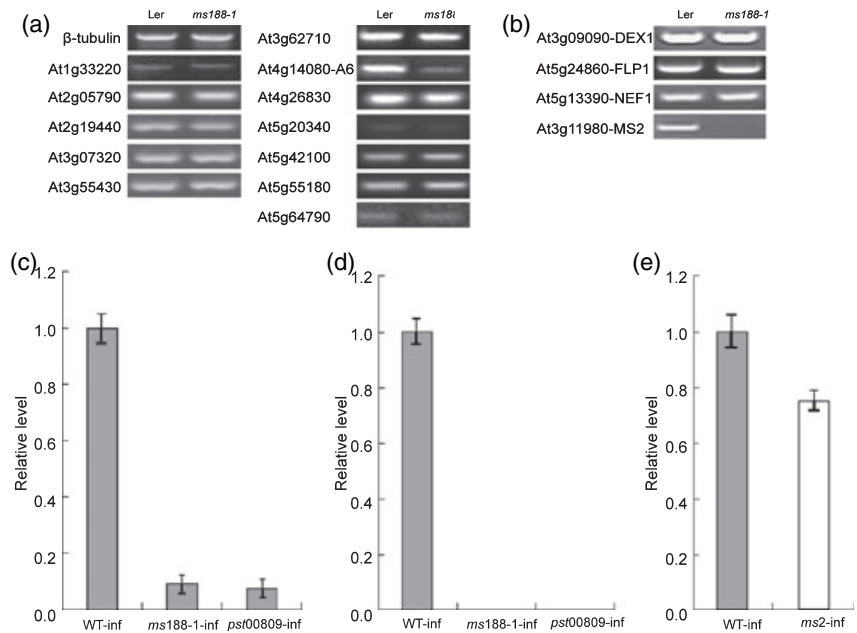**Figure 7.** *AtMYB103* regulates expression of downstream genes.
(a) RT-PCR analysis of 12 genes that encode β-1,3-glucanase in wild type and *ms188-1*.
(b) RT-PCR analysis of four genes involved in exine formation in the *ms188-1* mutants and in wild type.
(c) Real-time RT-PCR analysis of *A6* expression in wild-type and mutant (*ms188-1* and *pst00809*) backgrounds.
(d) Real-time RT-PCR analysis of *MS2* expression in wild-type (Ler), and mutant (*ms188* and *pst00809*) inflorescences.
(e) Real-time RT-PCR analysis of *AtMYB103* in both wild-type and *ms2* backgrounds. WT-inf, wild-type inflorescences; *ms188-1*-inf, *ms188-1* inflorescences; *pst00809*-inf, *pst00809* inflorescences; *ms2*-inf, *ms2* inflorescences.

AtMYB103 regulates tapetum development

In Arabidopsis, each lobe of the anther comprises four distinct sporophytic layers. The tapetum is the innermost of these four layers and comes in direct contact with the developing gametophyte (Sanders *et al.*, 1999). During anther development, tapetal cells become secretory type cells to provide the nutrition critical for pollen development (Raghavan, 1989; Stevens and Murray, 1981). In transgenic lines with reduced *AtMYB103* transcript levels, the tapetum cytoplasmic components disintegrated earlier, without releasing small oil bodies, plastids and vesicles (Higginson *et al.*, 2003). Our data also suggested that *AtMYB103* knock-out results in early tapetum degeneration.

During anther development, tapetal cell walls break down when tapetal cells become polar secretary-type cells (Stevens and Murray, 1981). In *ms188*, the tapetal cell walls remain intact late in anther development. Given that most of the callose had dissolved by the late stage of the *ms188* anther, this indicates that the tapetum may continue to secret some callase from the tapetum, and that the remaining tapetal cell wall may not completely prevent tapetum secretary activity. No gene or enzyme has yet been reported to be involved in tapetal cell wall degradation. Future functional analysis of AtMYB103, an MYB transcription factor, should facilitate the identification of genes coding for tapetal cell wall degradation enzymes.

AtMYB103 regulates A6 transcription during the callose dissolution

In anther development the tapetum releases callase to dissolve callose, and microspores are released from tetrads. Callose is mainly composed of β-1,3-glucan, suggesting that callase is a β-1,3-glucanase or a complex mainly composed of β-1,3-glucanase. Although several candidate β-1,3-glucanase encoding genes have been reported (Bucciaglia and Smith, 1994; Hird *et al.*, 1993), none has been confirmed to be a callase. Given that *AtMYB103* regulated callose dissolution, *ms188* provided an experimental approach to identify which gene was a callase-specific gene. Both RT-PCR and real-time RT-PCR analysis showed reduced *A6* expression in the *ms188* background. The expression level of the *A6* gene was in agreement with the partial degradation of callose in *ms188*. This indicates that *A6* may be a callase or a part of the callase enzyme complex, as suggested by Hird *et al.* (1993). Future identification of *A6* knock-out plants should help to confirm its role as a callase.

AtMYB103 *is required for the expression of* MS2 *to regulate exine formation*

Sporopollenin is the major constituent of the exine (Scott, 1994) and is formed by a series of related polymers derived from long-chain fatty acids, oxygenated aromatic rings and phenylpropanoids (Piffanelli *et al.*, 1998; Scott, 1994). Four genes have been reported to be involved in pollen exine development. *MS2* encodes a putative fatty acid reductase that catalyzes fatty acyl groups to fatty alcohol groups, and that may be involved in sporopollenin synthesis (Aarts *et al.*, 1997). The remaining three genes, *FLP1*, *DEX1* and *NEF1*, have been shown to play roles in exine pattern formation (Ariizumi *et al.*, 2003, 2004; Paxson-Sowders *et al.*, 2001). In *ms2* male sterile mutants, pollen development was arrested and no thick exine wall

deposition was observed. The *ms188* phenotype was similar to *ms2*. Both mutants were male sterile with few, defective pollen grains, and did not display exine formation. RT-PCR and real-time RT-PCR analysis demonstrated that the *MS2* gene acts downstream of *AtMYB103*. These data suggested both genes belonged to the same pathway. In order to identify if *AtMYB103* directly regulates the *MS2* gene, a yeast one-hybrid assay was employed. AtMYB103 did not bind to the 1.1-kb promoter region of the *MS2* gene (data not shown). This suggests that regulation between *AtMYB103* and *MS2* may be indirect. However, we cannot exclude the possibility that *AtMYB103* directly regulates *MS2* by binding its intron or 3′ regions.

AtMYB103 *and the* MS1 *gene*

In Arabidopsis, *MS1* plays an important function in late tapetum development and pollen wall formation. It encodes a nuclear protein with a PHD-finger motif and is involved in pollen development as a regulating factor (Wilson *et al.*, 2001). The electron microscopy experiments showed a complete lack of an exine layer on the surface of *ms188* pollen grains. Meanwhile, an irregular-shaped exine layer was formed in the *ms1* mutant, although the defected pollen grains were degraded before anther dehiscence (Vizcay-Barrena and Wilson, 2006). However, both *ms1* and *ms188* showed similar premature degeneration of tapetal cells. Our preliminary results showed that *MS1* expression was dramatically reduced in *ms188-1* inflorescences compared with those of wild type (Figure S2). On the other hand, the expression level of the *AtMYB103* gene was obviously ascended in *ms1* young and old anthers based on the microarray data from the Genevestigator database (http://www.genevestigator.ethz.ch). These results suggest that *AtMYB103* is likely to act upstream of the *MS1* gene in the genetic pathway of Arabidopsis anther development.

AtMYB103 *and trichome development*

Previous work examining *AtMYB103* function using antisense and sense technologies to downregulate its expression in transgenic plants suggested that disruption of *AtMYB103* expression may produce trichrome defects (Higginson *et al.*, 2003). The majority of rosette leaf adaxial surface trichromes were four-branched in the transgenic plants, rather than three-branched as in wild-type plants. Additionally, trichomes of transgenic plants were larger than those in the wild type. In the current study, the majority of the trichomes on the adaxial surface of rosette leaves of all three knock-out lines were three-branched (Table 1) and normal in size (data not shown), similar to wild-type trichomes. Thus, contrary to the findings of Higginson *et al.* (2003), the present results suggest that

Table 1 Trichome branching in rosette leaves from wild-type and mutant plants

Genotype	Trichome branching points[a]					Total[b]
	1	2	3	4	>5	
Wild-type	0	9.4	85.4	5.1	0.1	649
ms188-1	0.3	8.2	87.1	4.1	0.3	340
ms188-2	0	5.5	91.2	3.3	0	307
Wild-type (No-0)	0.2	16.3	83.5	0	0	575
pst00809 (No-0)	0.3	20.7	79.0	0	0	381

[a]Percentage of trichomes with the indicated number of branching points on the 4th and 5th rosette leaves.
[b]Total trichomes counted.

AtMYB103 is not crucial for trichome morphology (branching and size) in Arabidopsis. The trichome defect in the previous report was likely to be caused by secondary effects of the manipulation, rather than directly by down-regulation of *AtMYB103*.

Experimental procedures

Plant material

Arabidopsis mutants *ms188-1* and *ms188-2* (Landsberg *erecta*) were screened using an EMS mutagenesis strategy. Prior to phenotypic analysis, *ms188* was backcrossed to wild-type L*er* either three or four times. Seeds were sown on vermiculite and allowed to vernalize for 3 days at 4°C. Plants were grown at 22°C under a 16-h light/8-h dark photoperiod. A transposon tagged line of *AtMYB103* (pst00809) was purchased from the RIKEN mutant collection (http://rarge.gsc.riken.jp) (Seki *et al.*, 1998, 2002).

Mapping and cloning of MS188

Simple sequence length polymorphism (SSLP) and In/Del markers were used for first-pass mapping to localize *MS188* within the genome. For fine mapping, a total of 2135 F2 mutant plants from a cross between *ms188* (ecotype Ler) and Col were identified and used to prepare DNA for PCR-based mapping with SSLP and In/Del markers. The candidate gene was amplified from both the *ms188* and wild-type genomic DNA using primers 188GF (5′-TTAAGT AAAGAGTAATCAAATCG-3′) and 188GR (5′-CCAATGTTTAACTACC AATGTG-3′), and PCR products were sequenced directly.

MS188 *complementation experiment*

A 3611-bp genomic DNA fragment containing the predicted promotor, transcription region, and the 3′ untranslated region of *At-MYB103* was amplified using the LA Taq DNA polymerase PCR kit (Takara, http://www.takara-bio.com) with the gene-specific primers, 5′-CAAGTCAAGACAAATAGCAAAC-3′ and 5′-AGTAAGAATTCC TTTTCTTTCAC-3′. PCR product was cloned into pCAMBIA1300 binary vector (CAMBIA, http://www.cambia.org.au) and introduced into *ms188* heterozygous plants using the floral-dip method (Clough and Bent, 1998). Seeds were selected using 20 mg l⁻¹ hygromycin. The T1 lines were genotyped to identify homozygous *ms188* plants with the In/Del markers MDA7 and K24C1.

Light microscopy

Flower buds at different developmental stages were fixed overnight in FAA [ethanol 50% (v/v), acetic acid 5.0% (v/v) and formaldehyde 3.7% (v/v)], dehydrated in a graded ethanol series (50% twice, 60%, 70%, 80%, 90%, 95% and 100% twice), transferred to xylene and embedded in Spurr's epoxy resin. Thin sections (1 μm) were cut on a Powertome XL (RMC Products, http://www.rmcproducts.com) using glass knives, and were heat fixed to glass slides. Before staining with toluidine blue, sections were incubated in a saturated solution of sodium medium methoxide (2 min). Stained sections were rinsed in pure water three times and air dried. Bright-field photographs of the anther cross-sections were taken using an Olympus DX51 digital camera (http://www.olympus-global.com). Photographs presented here are representative of pollen development from at least five individual plants and show typical results. For examination of callose, sections were stained with 0.05% (w/v) analine blue in 0.067 M phosphate buffer (pH 8.5), and viewed under UV illumination.

Scanning electron microscopy

Individual wild-type and *ms188* anthers and pollen grains were collected from fresh dehiscence flowers during each of the 13 stages of anther development and were mounted on SEM stubs. Mounted samples were coated with palladium-gold in a sputter coater (pattern) and examined by SEM (JSM-840; JEOL, http://www.jeol.com) with an acceleration voltage of 15 kV. Photographs were taken using Haiou 120 film.

Transmission electron microscopy

Arabidopsis buds from the inflorescence were dissected on ice on an ice-cold drop of 2.5% glutaraldehyde (v/v) in 0.1 M phosphate buffer (pH 7.2). Dissected buds were transferred to a vial containing ice-cold vacuum-filtered fixative, then transferred to fresh fixative and fixed (4 h) on ice with gentle shaking. Buds were then washed twice in 0.1 M phosphate buffer (pH 7.2) before the addition of aqueous osmium tetroxide (final concentration of 1%). The material was post-fixed (2 h), the osmium tetroxide removed and the samples were dehydrated through 30-min exposures to a series of acetone/water mixtures (50%, 75%, 85%, 90%, 95% and three times 100% acetone). Flower buds were subsequently transferred to a 1:1 dry acetone:resin mix ('Hard Plus' Embedding Resin, TAAB premix kit; TAAB, http://www.taab.co.uk) on a rotator (12 h) and infiltrated in a 1:3 dry acetone: resin mix for an additional 12 h before transferring to freshly mixed resin. Following two fresh resin changes, the material was polymerized in molds (60°C, 24 h). Ultrathin sections (90–100 nm thick) were cut using diamond knives, and stained with uranyl acetate and lead citrate on an Ultrastainer, and were viewed in a Hitachi H-600 transmission electron microscope (Hitachi, http://www.hitachi.com).

Protein localization

Cellular localization of protein was examined by transient expression of the AtMYB103-GFP fusion protein. The complete *AtMYB103* coding sequence was amplified by PCR using two oligonucleotide primers, 5'-AGATCTGGGTCGGATTCCATGTTGTGAA-3' and 5'-ACTAGTAACCATATGATTGATGAGATC-3'. *AtMYB103* cDNA was cloned downstream of the 35S promoter of the cauliflower mosaic virus and was in frame with the GFP gene in the transient expression

vector pCAMBIA1302 (CAMBIA; http://www.cambia.org.au). The pCAMBIA1302-AtMYB103-GFP plasmid was delivered into onion epidermal cells using a Biolistic PDS-1000/He gene gun system (Bio-Rad, http://www.bio-rad.com). Bombarded samples were kept overnight at 26°C and observed by a ZEISS Confocal Laser Scanning Microscope (LSM 5 PASCAL; ZEISS, http://www.zeiss.com).

RNA extraction and real-time RT-PCR

Total RNA was isolated from floral tissue of mature soil-grown Arabidopsis plants using a Trizol kit (Invitrogen, http://www.invitrogen.com). First-strand cDNA was synthesized from 5 μg of RNA using poly (dT$_{12-18}$) primer, avian myeloblastosis virus reverse transcriptase and accompanying reagents for 60 min at 42°C; the synthesized cDNAs were used as PCR templates. PCR was performed for 30 cycles (real-time PCR for 40 cycles) (94°C, 30 sec; 54°C, 30 sec; 72°C, 30 sec). Real-time RT-PCR primers for *MS2* (AT3 G11980) were 5'-CTGCTGCT AATACAACCT-3' and 5'-TGCT-ATACAATCTCCCATA-3', for *A6* (AT4 G14080) 5'-TACCTAAACC-GACGAACA-3' and 5'-ATGCCAATAAATG GAGAC-3', for *AtMYB103* (AT5 G56110) 5'-GAAGAAGAAGTTGTC AGGAA-3', and 5'-GTGAG-CAAGTGAAGCATCT-3', β-tubulin (AT5 G23860) 5'-GATTTCAAA-GATTAGGGAAGAGTA-3' and 5'-GTTCTGAAGCAAATGTCATAG-AG-3'; β-tubulin was used as control. RT-PCR primers are indexed in Table S3.

Supplementary Material

The following supplementary material is available for this article online:

Figure S1. Alignment of the amino acid sequence of nine MYB genes in different species.
Figure S2. Real-time RT-PCR analysis of *MS1* in both wild-type and *ms188-1* backgrounds.
Table S1. List of molecular markers used for first-pass mapping.
Table S2. List of molecular markers used for fine-scale mapping.
Table S3. List of RT-PCR primers.
This material is available as part of the online article from http://www.blackwell-synergy.com

References

Aarts, M.G., Dirkse, W.G., Stiekema, W.J. and Pereira, A. (1993) Transposon tagging of a male sterility gene in *Arabidopsis*. *Nature*, **363**, 715–717.

Aarts, M.G., Hodge, R., Kalantidis, K., Florack, D., Scott, R. and Pereira, A. (1997) The *Arabidopsis* MALE STERILITY 2 protein shares similarity with reductases in elongation/condensation complexes. *Plant J.* **12**, 615–623.

Ariizumi, T., Hatakeyama, K., Hinata, K., Sato, S., Kato, T. and Toriyama, K. (2003) A novel male-sterile mutant of *Arabidopsis*

thaliana, faceless pollen-1, produces pollen with a smooth surface and an acetolysis-sensitive exine. *Plant Mol. Biol.* **53**, 107–116.

Ariizumi, T., Hatakeyama, K., Hinata, K., Inatsugi, R., Nishida, I., Sato, S., Kato, T., Tabata, S. and Toriyama, K. (2004) Disruption of the novel plant protein NEF1 affects lipid accumulation in the plastids of the tapetum and exine formation of pollen, resulting in male sterility in *Arabidopsis thaliana*. *Plant J.* **39**, 170–181.

Bucciaglia, P.A. and Smith, A.G. (1994) Cloning and characterization of Tag1, a tobacco anther β-1,3-glucanase expressed during tetrad dissolution. *Plant Mol. Biol.* **24**, 903–914.

Clough, S.J. and Bent, A.F. (1998) Floral dip: a simplified method for *Agrobacterium*-mediated transformation of *Arabidopsis thaliana*. *Plant J.* **16**, 735–743.

Fitzgerald, M.A. and Knox, R.B. (1995) Initiation of primexine in freeze-substituted microspores of *Brassica campestris*. *Sex. Plant Reprod.* **8**, 99–104.

Goldberg, R.B., Beals, T.P. and Sanders, P.M. (1993) Anther development: basic principles and practical applications. *Plant Cell*, **5**, 1217–1229.

Heslop-Harrison, J. (1963) An ultrastructural study of pollen wall ontogeny in *Silene pendula*. *Grana Palynologica.* **4**, 7–24.

Higginson, T., Li, S.F. and Parish, R.W. (2003) *AtMYB103* regulates tapetum and trichome development in *Arabidopsis thaliana*. *Plant J.* **35**, 177–192.

Hird, D.L., Worrall, D., Hodge, R., Smartt, S., Paul, W. and Scott, R. (1993) The anther-specific protein encoded by the *Brassica napus* and *Arabidopsis thaliana* A6 gene displays similarity to β-1,3-glucanase. *Plant J.* **4**, 1023–1033.

Jander, G., Norris, S.R., Rounsley, S.D., Bush, S.F., Levin, I.M. and Last, R.L. (2002) *Arabidopsis* map-based cloning in the post-genome era. *Plant Physiol.* **129**, 440–450.

Li, S.F., Higginson, T. and Parish, R.W. (1999) A novel MYB-related gene from *Arabidopsis thaliana* expressed in development anthers. *Plant Cell Physiol.* **40**, 343–347.

Millar, A.A. and Gubler, F. (2005) The *Arabidopsis GAMYB-like* genes, *MYB33 and MYB65*, are microRNA-regulated genes that redundantly facilitate anther development. *Plant Cell*, **17**, 705–721.

Paxson-Sowders, D.M., Dodrill, C.H., Owen, H.A. and Makaroff, C.A. (2001) *DEX1*, a novel plant protein, is required for exine pattern formation during pollen development in *Arabidopsis*. *Plant Physiol.* **127**, 1739–1749.

Piffanelli, P., Ross, J.H.E. and Murphy, D.J. (1998) Biogenesis and function of the lipidic structures of pollen grains. *Sex. Plant Reprod.* **11**, 65–80.

Preston, J., Wheeler, J., Heazlewood, J., Li, S.F. and Parish, R.W. (2004) AtMYB32 is required for normal pollen development in *Arabidopsis thaliana*. *Plant J.* **40**, 979–995.

Raghavan, V. (1989) mRNAs and a cloned histone gene are differentially expressed during anther and pollen development in rice (*Oryza sativa* L.). *J. Cell Sci.* **92**, 217–229.

Sanders, P.M., Bui, A.Q., Weterings, K., McIntire, K.N., Hsu, Y.C., Lee, P.Y., Truong, M.T., Beals, T.P. and Goldberg, R.B. (1999) Anther developmental defects in *Arabidopsis thaliana* male-sterile mutants. *Sex. Plant Reprod.* **11**, 297–322.

Scott, R.J. (1994) Pollen exine: the sporopollenin enigma and the physics of pattern. In *Molecular and Cellular Aspects of Plant Reproduction* (Scott, R.J. and Stead, M.A., eds). Cambridge, UK: University Press, pp. 49–81.

Scott, R.J., Spielmana, M. and Dickinsonb, H.G. (2004) Stamen structure and function. *Plant Cell*, **16**, 46–60.

Seki, M., Carninci, P., Nishiyama, Y., Hayashizaki, Y. and Shinozaki, K. (1998) High-efficiency cloning of *Arabidopsis* full-length cDNA by biotinylated CAP trapper. *Plant J.* **15**, 707–720.

Seki, M., Narusaka, M., Kamiya, A. *et al.* (2002) Functional annotation of a full-length *Arabidopsis* cDNA collection. *Science*, **296**, 141–145.

Steer, M.W. (1977) Differentiation of the tapetum in Avena. I. The cell surface. *J. Cell Sci.* **25**, 125–138.

Steiglitz, H. (1977) Role of β-1,3-glucanase in postmeiotic microspore release. *Dev. Biol.* **57**, 87–97.

Steiglitz, H. and Stern, H. (1973) Regulation of β-1,3-glucanase activity in developing anthers of Lilium. *Dev. Biol.* **34**, 169–173.

Steiner-lange, S., Unte, U.S., Eckstein, L., Yang, C., Wilson, Z.A., Schmelzer, E., Dekker, K. and Saedler, H. (2003) Disruption of *Arabidopsis thaliana* MYB26 results in male sterility due to non-dehiscent anthers. *Plant J.* **34**, 519–528.

Stevens, V.A. and Murray, B.G. (1981) Studies on heteromorphic self-incompatibility systems: the cytochemistry and ultrastructure of the tapetum of *Primula obconica*. *J. Cell Sci.* **50**, 419–431.

Vizcay-Barrena, G. and Wilson, Z.A. (2006) Altered tapetal PCD and pollen wall development in the *Arabidopsis ms1* mutant. *J. Exp. Bot.* **57**, 2709–2717.

Wilson, Z.A., Morroll, S.M., Dawson, J., Swarup, R. and Tighe, P.J. (2001) The *Arabidopsis MALE STERILITY1* (*MS1*) gene is a transcriptional regulator of male gametogenesis, with homology to the PHD-finger family of transcription factors. *Plant J.* **28**, 27–39.

Yang, S., Sweetman, J.P., Amirsadeghi, S., Barghchi, M., Huttly, A.K., Chung, W.I. and Twell, D. (2001) Novel anther-specific myb genes from tobacco as putative regulators of phenylalanine ammonia-lyase expression. *Plant Physiol.* **126**, 1738–1753.

Zhang, P.F., Chopra, S. and Peterson, T. (2000) A segmental gene duplication generated differentially expressed myb-homologous genes in maize. *Plant Cell*, **12**, 2311–2322.

Zhu, Q.H., Ramm, K., Shivakkumar, R., Dennis, E.S. and Upadhyaya, N.M. (2004) The *ANTHER INDEHISCENCE1* gene encoding a single MYB domain protein is involved in anther development in rice. *Plant Physiol.* **135**, 1514–1525.